### Title

A Dinuclear Mechanism Implicated in Controlled Carbene Polymerization




### Journal

Journal of the American Chemical Society, 141(16)

### ISSN

0002-7863



### Authors

Zhukhovitskiy, Aleksandr V
Kobylianskii, Ilia J
Thomas, Andy A
et al.



### Publication Date

2019-04-24

### DOI

10.1021/jacs.9b01532

Peer reviewed

Published in final edited form as:

*J Am Chem Soc*. 2019 April 24; 141(16): 6473–6478. doi:10.1021/jacs.9b01532.

# A Dinuclear Mechanism Implicated in Controlled Carbene Polymerization

**Aleksandr V. Zhukhovitskiy**[†,‖], **Ilia J. Kobylianskii**[†,‖], **Andy A. Thomas**[‡,⊥], **Austin M. Evans**[§], **Connor P. Delaney**[‡], **Nathan C. Flanders**[§], **Scott E. Denmark**[‡], **William R. Dichtel**[§], and **F. Dean Toste**[*,†]

[†]Department of Chemistry, University of California, Berkeley, California 94720, United States

[‡]Roger Adams Laboratory, Department of Chemistry, University of Illinois, Urbana, Illinois 61801, United States

[§]Department of Chemistry, Northwestern University, Evanston, Illinois 60208, United States

## Abstract

Carbene polymerization provides polyolefins that cannot be readily prepared from olefin monomers; however, controlled and living carbene polymerization has been a long-standing challenge. Here we report a new class of initiators, ($\pi$-allyl)palladium carboxylate dimers, which polymerize ethyl diazoacetate, a carbene precursor in a controlled and quasi-living manner, with nearly quantitative yields, degrees of polymerization >100, molecular weight dispersities 1.2–1.4, and well-defined, diversifiable chain ends. This method also provides block copolycarbenes that undergo microphase segregation. Experimental and theoretical mechanistic analysis supports a new dinuclear mechanism for this process.

Cooperativity among two or more metal centers is an evolution-validated tactic to catalyze challenging chemical transformations. Such multinuclear catalysis is at work, for instance, in the hydrolysis of urea by the urease enzyme: two Ni(II) centers bridged by a carboxylate ligand cooperatively direct hydroxide addition to an activated urea (Figure 1A).[1] Outside of the context of enzymatic chemistry, multinuclear catalysis has received far less attention than single-site catalysis, but its power is undeniable for molecular synthesis and polymerization,[2,3] including the globally significant Fischer-Tropsch reaction (FTR) (Figure 1A).[4] Here we report evidence of dinuclear catalysis operative in the quasi-living and controlled carbene polymerization to produce densely substituted block-*co*-polyolefins that cannot be prepared from olefin monomers.

[*]**Corresponding Author** fdtoste@berkeley.edu.

[⊥]**Present Address** A.A.T.: Department of Chemistry, Massachusetts Institute of Technology, Cambridge, Massachusetts 02139, United States.

[‖]A.V.Z. and I.J.K. contributed equally.

ASSOCIATED CONTENT

Supporting Information

The Supporting Information is available free of charge on the ACS Publications website at DOI: 10.1021/jacs.9b01532.

Materials and methods, synthetic and characterization procedures, supplementary text and figures, and spectral data (PDF)

Coordinates for DFT-computed structures (PDF)

The authors declare no competing financial interest.

Pioneering work by the groups of Ihara and de Bruin demonstrated that polymerization of ethyl diazoacetate (EDA) and other $\alpha$-diazocarbonyl compounds, functional carbene precursors, could be initiated by homogeneous palladium[5,6] and rhodium[6–19] species (Figure 1B): the former generally yield atactic polymers, and the latter, syndiotactic ones.[5,20] Yet, controlled and living polymerization of $\alpha$-diazocarbonyl compounds has been a crucial challenge: in one case control could be attained by alcohol/water-mediated chain transfer,[14] and only two reported systems exhibited control and living-ness,[21–23] of which one[21,22] did not generalize beyond cyclotriphosphazene-containing monomers. Furthermore, formation of maleate and fumarate esters and analogous carbene dimers plagues most[15] existing methods and compromises the polymer yield (Figure 1B).[5,7,11,15] Although theoretical and mechanistic studies have been carried out for some initiators, particularly based on Rh,[15,18,24] numerous aspects of initiation and propagation remain ill-defined, which has inhibited progress.

Inspired by our recent studies into migratory insertion in carbenoid gold intermediates,[25] we began our investigation with ($\pi$-allyl)palladium chloride dimer (l), known to initiate the polymerization of EDA.[26] We hypothesized that the low-moderate yields of polymer resulted from the low nucleophilicity and Lewis basicity of the chloride ligand, detrimental to its migratory aptitude. This factor, in addition to suboptimal reaction conditions, could be responsible for reported chain termination, poor control of the number-average molecular weight ($M_n$) and end-groups, and broad dispersity (D) known for 1 (Figure 1B).[26] We hypothesized that replacing the chloride ligands with the more nucleophilic and Lewis basic carboxylates would accelerate initiation relative to propagation, which would suppress maleate/fumarate formation, reduce Đ, and improve chain end control.

Comparison of 1 and ($\pi$-allyl)palladium acetate dimer[27–29] (2), as well as ($\pi$-allyl)palladium methacrylate dimer (3) in the polymerization of EDA and 2,2,2-trifluoroethyl diazoacetate (TFEDA)[30] under equivalent conditions revealed that, as anticipated, in the presence of 2 and 3, both monomers were polymerized in nearly quantitative yield, while **1** afforded low yields of corresponding polycarbenes and mostly produced maleate and fumarate esters (Figure 2A). Matrix-assisted laser desorption ionization time-of-flight mass spectrometry (MALDI-TOF MS) confirmed that the polymer chains were virtually uniformly carboxylate-initiated and hydrogen-terminated, the latter presumably generated through protodepalladation upon exposure to air (Figure 2B, Supporting Information (SI), Figures S1 and S2). In some cases, small amounts of OH-initiated chains were observed (Figure 2B, inset), due to incomplete elimination of water from the reaction mixture. Use of both 2 and 2-$d_6$, wherein the acetate moieties were deuteriumlabeled, facilitated these assignments and indicated that protodepalladation was the only mode of termination operative under these conditions (SI, Figure S2). Therefore, the controlled installation of distinct chain ends is another advantage of this method.

Furthermore, in anhydrous fluorobenzene at 0 °C, excellent $M_n$-control and low Đ(≤1.3) in the polymerization of EDA were observed for 2 up to an EDA:initiator ratio of ~150:1; this control is in stark contrast to 1 (Figure 2C and SI, Figure S3). As a testament to the robustness of the present method, high polymers ($M_n$ ≈ 25000 (degree of polymerization (DP) ≈ 290) and Đ≈ 1.42) were readily accessed in the polymerization of EDA. Notably, the

observed $M_n$ values were close to the theoretical ones based on the ratio of the monomer to the dinuclear initiator, which indicated that half of the available Pd sites initiated chain growth, either due to incomplete initiator consumption, initiator decomposition, or a dinuclear polymerization pathway. From variable temperature (VT) $^1$H nuclear magnetic resonance (NMR) spectroscopy (in DCM-$d_2$ at −40 °C), we also noted that the methyl resonance from the acetate groups of 2 ("a" in Figure 2D) was completely consumed and transformed into three resonances upfield of "a"; one of these resonances ("d" in Figure 2D) was broad, integrated to ~ half of the original methyl resonance from 2, and based on diffusion ordered spectroscopy (DOSY, SI, Figure S4) was assigned to the chain end of the polymer. DP determined via end-group analysis was 47, nearly identical to $[EDA]_o$:$[2]_o$ ratio of 50. These results supported a dinuclear mechanism, wherein one of the acetate ligands in 2 initiates the polymer growth through migratory insertion, while the other remains ancillary and bridges the two Pd centers.

VT $^1$H NMR kinetics analysis is fully consistent with this mechanism (SI, Figures S5–S9 and "VT NMR Kinetics" in the SI). We find that the decay profile of 2 exhibits first-order behavior; meanwhile, EDA is consumed with mixed first-order/second-order kinetics that give rise to a mixed exponential/double exponential rate law (SI, Figure S6):

$$[2] = [2]_o e^{-A_1 \varphi \times t} \quad (1)$$

$$[EDA] = [EDA]_o e^{-[2]_o \times \left( A_2 t + \frac{-2A_1 + A_2}{A_1 \varphi} \left( e^{-A_1 \varphi \times t} - 1 \right) \right)} \quad (2)$$

wherein [EDA] and [2] are the concentrations of EDA and 2, respectively, at time $t$, $[EDA]_o$, and $[2]_o$ are the corresponding initial concentrations, $A_1 = 1.64 \pm 0.10 \times 10^{-1}\ M^{-1}\ s^{-1}$ and $A_2 = 8.76 \pm 0.09 \times 10^{-2}\ M^{-1}\ s^{-1}$ are measures of initiation and propagation rate constants, and $\varphi = 2.3 \pm 0.2 \times 10^{-2}$ and $\varphi > 1$ (SI, Figures S7–S9 and "VT NMR Kinetics" in the SI) are measures of selectivity of acetate and enolate migration, respectively, over the formation of diethyl maleate and fumarate.

From rapid injection NMR spectroscopy (RI-NMR)[34,35] in toluene-d8 at −20 °C (Figure 3, SI, Figures S10–S19, Tables S2–S8, and "Rapid Injection NMR" section, SI), we concluded that initiation is substantially accelerated in the absolute sense for **2** compared to **1**: the former was completely consumed within ~2 min at −20 °C, while the latter has a $t_{1/2}$ = 4.4 ± 0.2 min. Additionally, we observed from RI-NMR that **1** catalyzed the dimerization of EDA more rapidly than does the propagating Pd-enolate species (formed via initiation with **2**). Thus, **2** initiates faster than **1**, and once initiation occurs, dimerization is outcompeted by propagation.

Theoretical analysis via density functional theory (DFT) also supported a dinuclear mechanism (Figure 4 and SI, Figure S20, "Computations" section, SI). We computed $\Delta H^{\ddagger}$ =

36.5 kcal/mol for the mononuclear initiation pathway for 2, wherein 2 first dissociates into two halves prior to carbene generation via rate-determining $N_2$ elimination; on the other hand, the dinuclear pathway has $\Delta H^{\ddagger}$ = 22.1 kcal/mol, i.e., 14.4 kcal/mol lower (a similar disparity is observed for **1**). Furthermore, in accord with experimental evidence, theory dictates that one of the acetate ligands in 2 migrates and generates a $Pd_2$-enolate species, while the other acetate remains ancillary, holding the two Pd centers in proximity.[36]

Beyond improved control, the polymerization of EDA with 2 was also found to be quasi-living based on the chain lifetime test, wherein progressively greater time intervals separated the addition of a second batch of 50 equiv EDA from the addition of 2 to the first. As shown in Figure 5A, $M_n$ hardly changed (~4–8%) even with a 16 min interval, and D was essentially constant with time between batches, although the first batch of EDA is completely consumed within ~4.5 min (SI, Figures S20 and S21, and "DMAP-quenching experiments" section, SI). In other words, nearly all of the chains initiated by **2** remain alive during the course of at least 16 min; however, because we do observe a small drop in $M_n$, we believe that this method is best described as quasi-living.

The reality of a quasi-living carbene polymerization for readily available monomers like EDA opens the door to the synthesis of a diverse range of densely functionalized block copolymers. Similarly to 2, quasi-living behavior and fine chain-end and $M_n$ control were also observed for ($\pi$-allyl)palladium pivalate dimer (**4**) (SI, Figure S23), and this initiator was utilized to test the ability to form block copolymers (Figure 5B). Indeed, polymerization of 50 equiv of EDA, followed by addition of 50 equiv of TFEDA, led to nearly perfect chain extension and the formation of diblock copolymers as judged by GPC-viscometry (SI, Figure S24), as well as complete dissolution of the polymer in $CDCl_3$, in which the TFEDA-derived homopolymers are only marginally soluble.

Furthermore, sequential enchainment of 50 equiv of EDA and 70 equiv of TFEDA (SI, Figure S25) produced materials that exhibited efficient microphase segregation typical of block copolymers. Small-/wide-angle X-ray scattering (SAXS/WAXS) (Figure 5B) revealed a scattering peak pattern of (1q, 2q, 3q), indicative of a well-ordered lamellar morphology in the films of this polymer produced by slow THF evaporation. Peak broadening was attributed to finite grain size effects, and Scherrer analysis was used to calculate a grain size of 62 $\mu$m based on this assumption.[37] Furthermore, the value of $q$ = 0.018 $Å^{-1}$ corresponded to a characteristic lamellar spacing of 350 A. The end-to-end distance of the fully stretched out block copolymers of DP ~ 175 (based on Figure 2C and relative ratio of two blocks) is estimated to be 220 Å ("End-to-End Distance" section, SI), which translates to a $d$-spacing of 440 Å. These numbers suggest that the polycarbene backbones are highly extended rather than coiled, as recently described for atactic homopolymers of benzyl diazoacetate.[38] Note also that compared to the corresponding homopolymer segments, the block copolymer appears to have similar thermal stability in air up to ~260 °C (SI, Figure S26).

Hence, we report an efficient, controlled, and quasi-living polymerization of EDA and block-co-polymerization of EDA and TFEDA enabled by a dinuclear mechanism. Although dinuclear polymerization of olefins is well-precedented,[3] as is the existence of bridging carbenes,[39–44] dinuclear reactivity in carbene polymerization has no precedent in

homogeneous catalysis. The mechanistic insights in this report, e.g., the ancillary nature of one of the carboxylates, and the stabilization of reactive intermediates by the two Pd centers, [45–49] will not only advance initiator design for carbene polymerization, but will also readily translate to catalysis as broadly defined.

## Supplementary Material

Refer to Web version on PubMed Central for supplementary material.

## ACKNOWLEDGMENTS

We thank the National Institute of Health (R35 GM118190) for support of this work. A.V.Z. is a Merck Fellow of the Life Sciences Research Foundation. I.J.K. is a Swiss National Science Foundation postdoctoral fellow. A.A.T. is an NIH NRSA fellow (1F32GM125163). AM.E. is supported by the NSF Graduate Research Fellowship under grant DGE-1324585, the Ryan Fellowship, and the Northwestern University International Institute for Nanotechnology. We thank B. Elling, J. Su, and Prof. Y. Xia at Stanford University for generously facilitating our use of the GPC-MALLS and MALDI-TOF. We thank Z. Zhou and R. Nichiporuk for assistance with HRMS and G. Sethi for assistance with TGA. This work made use of the UC Berkeley Catalysis Center, managed by M. Zhang, the College of Chemistry and QB-3 Institute NMR facilities, the Stanford University Mass Spectrometry facility, and the DuPont-Northwestern-Dow Collaborative Access Team (DND-CAT) located at Sector 5 of the Advanced Photon Source (APS). DND-CAT is supported by Northwestern University, E.I. DuPont de Nemours & Co., and The Dow Chemical Company. This research used resources of the Advanced Photon Source, a U.S. Department of Energy (DOE) Office of Science User Facility operated for the DOE Office of Science by Argonne National Laboratory under contract DE-AC02-06CH11357. Data was collected using an instrument funded by the National Science Foundation under award no. 0960140. Work at the Molecular Foundry was supported by the Office of Science, Office of Basic Energy Sciences, of the U.S. DOE under contract DE-AC02-05CH11231. DFT studies were conducted at the Molecular Graphics and Computation Facility, funded by NIH grant S10OD023532.

## REFERENCES

(1). Benini S; Rypniewski WR; Wilson KS; Miletti S; Ciurli S; Mangani S A New Proposal for Urease Mechanism Based on the Crystal Structures of the Native and Inhibited Enzyme from Bacillus Pasteurii: Why Urea Hydrolysis Costs Two Nickels. Structure 1999, 7, 205–216. [PubMed: 10368287]

(2). Pye DR; Mankad NP Bimetallic Catalysis for C—C and C—X Coupling Reactions. Chem. Sci 2017, 8, 1705–1718. [PubMed: 29780450]

(3). Delferro M; Marks TJ Multinuclear Olefin Polymerization Catalysts. Chem. Rev. 2011, 111, 2450–2485. [PubMed: 21329366]

(4). Gaube J; Klein HF Studies on the Reaction Mechanism of the Fischer—Tropsch Synthesis on Iron and Cobalt. J. Mol. Catal A: Chem. 2008, 283, 60–68.

(5). Ihara E; Itoh T; Shimomoto H Polymerization of Alkyl Diazoacetates Initiated with Pd Complexes. Macromol Symp. 2015, 349, 57–64.

(6). Ihara E; Shimomoto H, Polymerization of Diazoacetates: New Synthetic Strategy for C—C Main Chain Polymers. Polymer 2018 DOI: 10.1016/j.polymer.2018.11.049

(7). Hetterscheid DGH; Hendriksen C; Dzik WI; Smits JMM; van Eck ERH; Rowan AE; Busico V; Vacatello M; Van Axel Castelli V; Segre A; Jellema E; Bloemberg TG; de Bruin B Rhodium-Mediated Stereoselective Polymerization of “Carbenes. J. Am. Chem. Soc. 2006, 128, 9746–9752. [PubMed: 16866530]

(8). Jellema E; Budzelaar PHM; Reek JNH; de Bruin B Rh-Mediated Polymerization of Carbenes: Mechanism and Stereoregulation. J. Am. Chem. Soc. 2007, 129, 11631–11641. [PubMed: 17715925]

(9). Jellema E; Jongerius AL; van Ekenstein GA; Mookhoek SD; Dingemans TJ; Reingruber EM; Chojnacka A; Schoenmakers PJ; Sprenkels R; van Eck ERH; Reek JNH; de Bruin B Rhodium-Mediated Stereospecific Carbene Polymerization: From Homopolymers to Random and Block Copolymers. Macromolecules 2010, 43, 8892–8903.

(10). Jellema E; Jongerius AL; Walters AJC; Smits JMM; Reek JNH; de Bruin B Ligand Design in Rh(diene)-Mediated “Carbene” Polymerization; Efficient Synthesis of High-Mass, Highly Stereoregular, and Fully Functionalized Carbon-Chain Polymers. Organometallics 2010, 29, 2823–2826.

(11). Finger M; Reek JNH; de Bruin B Role of β-H Elimination in Rhodium-Mediated Carbene Insertion Polymerization. Organometallics 2011, 30, 1094–1101.

(12). Franssen NMG; Remerie K; Macko T; Reek JNH; de Bruin B Controlled Synthesis of Functional Copolymers with Blocky Architectures via Carbene Polymerization. Macromolecules 2012, 45, 3711–3721.

(13). Suarez AIO; del Río MP; Remerie K; Reek JNH; de Bruin B Rh-Mediated C1-Polymerization: Copolymers from Diazo-esters and Sulfoxonium Ylides. ACS Catal. 2012, 2, 2046–2059.

(14). Walters AJC; Jellema E; Finger M; Aarnoutse P; Smits JMM; Reek JNH; de Bruin B Rh-Mediated Carbene Polymerization: From Multistep Catalyst Activation to Alcohol-Mediated Chain-Transfer. ACS Catal. 2012, 2, 246–260.

(15). Walters AJC; Troeppner O; Ivanovic-Burmazovic I; Tejel C; del Río MP; Reek JNH; de Bruin B Stereospecific Carbene Polymerization with Oxygenated Rh(diene) Species. Angew. Chem., Int. Ed. 2012, 51, 5157–5161.

(16). Franssen NMG; Ensing B; Hegde M; Dingemans TJ; Norder B; Picken SJ; Alberda van Ekenstein GOR; van Eck ERH; Elemans JAAW; Vis M; Reek JNH; de Bruin B On the “Tertiary Structure” of Poly-Carbenes; Self-Assembly of sp3-Carbon-Based Polymers into Liquid-Crystalline Aggregates. Chem. - Eur. J. 2013, 19, 11577–11589. [PubMed: 23852805]

(17). Franssen NMG; Reek JNH; de Bruin B A Different Route to Functional Polyolefins: Olefin-Carbene Copolymerisation. Dalton Trans 2013, 42, 9058–9068. [PubMed: 23361412]

(18). Walters AJC; Reek JNH; de Bruin B Computed Propagation and Termination Steps in [(Cycloocta-2,6-dien-1-yl)-RhIII(polymeryl)]+ Catalyzed Carbene Polymerization Reactions. ACS Catal. 2014, 4, 1376–1389.

(19). Tromp DS; Lankelma M; de Valk H; de Josselin de Jong E; de Bruin B. Aqueous Phase Separation Behavior of Highly Syndiotactic, High Molecular Weight Polymers with Densely Packed Hydroxy-Containing Side Groups. Macromolecules 2018, 51, 7248–7256. [PubMed: 30270941]

(20). Jellema E; Jongerius AL; Reek JNH; de Bruin B C1 Polymerisation and Related C-C Bond Forming ‘Carbene Insertion’ Reactions. Chem. Soc. Rev. 2010, 39, 1706–1723. [PubMed: 20419216]

(21). Shimomoto H; Asano H; Itoh T; Ihara E Pd-initiated Controlled Polymerization of Diazoacetates with a Bulky Substituent: Synthesis of Well-defined Homopolymers and Block Copolymers with Narrow Molecular Weight Distribution from Cyclophosphazene-Containing Diazoacetates. Polym. Chem. 2015, 6, 4709–4714.

(22). Kato F; Chandra A; Tokita M; Asano H; Shimomoto H; Ihara E; Hayakawa T Self-Assembly of Hierarchical Structures Using Cyclotriphosphazene-Containing Poly(substituted methylene) Block Copolymers. ACS Macro Lett. 2018, 7, 37–41.

(23). Chu J-H; Xu X-H; Kang S-M; Liu N; Wu Z-Q Fast Living Polymerization and Helix-Sense-Selective Polymerization of Diazo-acetates Using Air-Stable Palladium(II) Catalysts. J. Am. Chem. Soc. 2018, 140, 17773–17781. [PubMed: 30488700]

(24). Xiao L; Li F; Li Y; Jia X; Liu L Kinetic Study of Carbene Polymerization of Ethyl Diazoacetate by Palladium and Rhodium Catalysts. RSC Adv. 2014, 4, 41848–41855.

(25). Zhukhovitskiy AV; Kobylianskii IJ; Wu C-Y; Toste FD Migratory Insertion of Carbenes into Au(III)-C Bonds. J. Am. Chem. Soc. 2018, 140, 466–474. [PubMed: 29260868]

(26). Ihara E; Akazawa M; Itoh T; Fujii M; Yamashita K; Inoue K; Itoh T; Shimomoto H π-AllylPdCl-Based Initiating Systems for Polymerization of Alkyl Diazoacetates: Initiation and Termination Mechanism Based on Analysis of Polymer Chain End Structures. Macromolecules 2012, 45, 6869–6877.

(27). Lupin MS; Robinson SD; Shaw BL Proceedings of the Eighth ICCC; Vienna, 1964; p 223.

(28). Robinson SD; Shaw BL Transition Metal-carbon Bonds: IV. Carboxylato-bridged n-allylic palladium(ll) Complexes. J. Organomet. Chem. 1965, 3, 367–370.

(29). Churchill M R; Mason, R Molecular Structure of π-allyl-palladium Acetate. Nature 1964, 204, 777.

(30). Shimomoto H; Kudo T; Tsunematsu S; Itoh T; Ihara E Fluorinated Poly(substituted methylene)s Prepared by Pd-Initiated Polymerization of Fluorine-Containing Alkyl and Phenyl Diazoacetates: Their Unique Solubility and Postpolymerization Modification. Macromolecules 2018, 51, 328–335.

(31). Konsler RG; Karl J; Jacobsen EN Cooperative Asymmetric Catalysis with Dimeric Salen Complexes. J. Am. Chem. Soc. 1998, 120, 10780–10781.

(32). Doyle MP; Duffy R; Ratnikov M; Zhou L Catalytic Carbene Insertion into C—H Bonds. Chem. Rev. 2010, 110, 704–724. [PubMed: 19785457]

(33). Ihara E; Ishiguro Y; Yoshida N; Hiraren T; Itoh T; Inoue K (N-Heterocyclic Carbene)Pd/Borate Initiating Systems for Polymerization of Ethyl Diazoacetate. Macromolecules 2009, 42, 8608–8610.

(34). Denmark SE; Williams BJ; Eklov BM; Pham SM; Beutner GL Design, Validation, and Implementation of a Rapid-Injection NMR System. J. Org. Chem. 2010, 75, 5558–5572. [PubMed: 20672809]

(35). Thomas AA; Denmark SE, Eliel Ernest, L., a Physical Organic Chemist with the Right Tool for the Job: Rapid Injection Nuclear Magnetic Resonance In Stereochemistry and Global Connectivity: The Legacy of Eliel Ernest L.; American Chemical Society: Washington DC, 2017; Vol. 2, pp 105–134.

(36). The shallow nature of the transition state (TS3) for this step, as well as the presence of structurally labile fragments, rendered its exact energy tedious to calculate; we estimated it at ~21.3 kcal/mol based on 0.02 A increment linear transit calculations at the same level of theory.

(37). Chintapalli M; Chen XC; Thelen JL; Teran AA; Wang X; Garetz BA; Balsara NP Effect of Grain Size on the Ionic Conductivity of a Block Copolymer Electrolyte. Macromolecules 2014, 47, 5424–5431.

(38). Shikinaka K; Suzuki K; Masunaga H; Ihara E; Shigehara K Stiff and Hierarchical Chain Nature of Atactic and Stereoregular Poly(substituted methylene)s. Polym. Int. 2018, 67, 495–499.

(39). Dai X; Warren TH Discrete Bridging and Terminal Copper Carbenes in Copper-Catalyzed Cyclopropanation. J. Am. Chem. Soc. 2004, 126, 10085–10094. [PubMed: 15303885]

(40). Badiei YM; Warren TH Electronic Structure and Electrophilic Reactivity of Discrete Copper Diphenylcarbenes. J. Organomet. Chem. 2005, 690, 5989–6000.

(41). Hofmann P; Shishkov IV; Rominger F Synthesis, Molecular Structures, and Reactivity of Mono- and Binuclear Neutral Copper(I) Carbenes. Inorg. Chem. 2008, 47, 11755–11762. [PubMed: 19053350]

(42). Laskowski CA; Hillhouse GL Synthesis and carbene-transfer reactivity of dimeric nickel carbene cations supported by N-heterocyclic carbene ligands. Chem. Sci. 2011, 2, 321–325.

(43). Maity AK; Zeller M; Uyeda C Carbene Formation and Transfer at a Dinickel Active Site. Organometallics 2018, 37, 2437–2441. [PubMed: 31080305]

(44). Schmidbaur H; Schier A Science of Synthesis; Thieme Chemistry, 2004; Vol. 3, p 692

(45). Haines BE; Berry JF; Yu J-Q; Musaev DG Factors Controlling Stability and Reactivity of Dimeric Pd(II) Complexes in C-H Functionalization Catalysis. ACS Catal 2016, 6, 829–839.

(46). Powers DC; Benitez D; Tkatchouk E; Goddard WA; Ritter T Bimetallic Reductive Elimination from Dinuclear Pd(III) Complexes. J. Am. Chem. Soc. 2010, 132, 14092–14103. [PubMed: 20858006]

(47). Powers DC; Xiao DY; Geibel MAL; Ritter T On the Mechanism of Palladium-Catalyzed Aromatic C-H Oxidation. J. Am. Chem. Soc. 2010, 132, 14530–14536. [PubMed: 20873835]

(48). Cook AK; Sanford MS Mechanism of the Palladium-Catalyzed Arene C-H Acetoxylation: A Comparison of Catalysts and Ligand Effects. J. Am. Chem. Soc. 2015, 137, 3109–3118. [PubMed: 25706227]

(49). Paton RS; Brown JM Dinuclear Palladium Complexes—Precursors or Catalysts? Angew. Chem. Int. Ed. 2012, 51, 10448–10450.

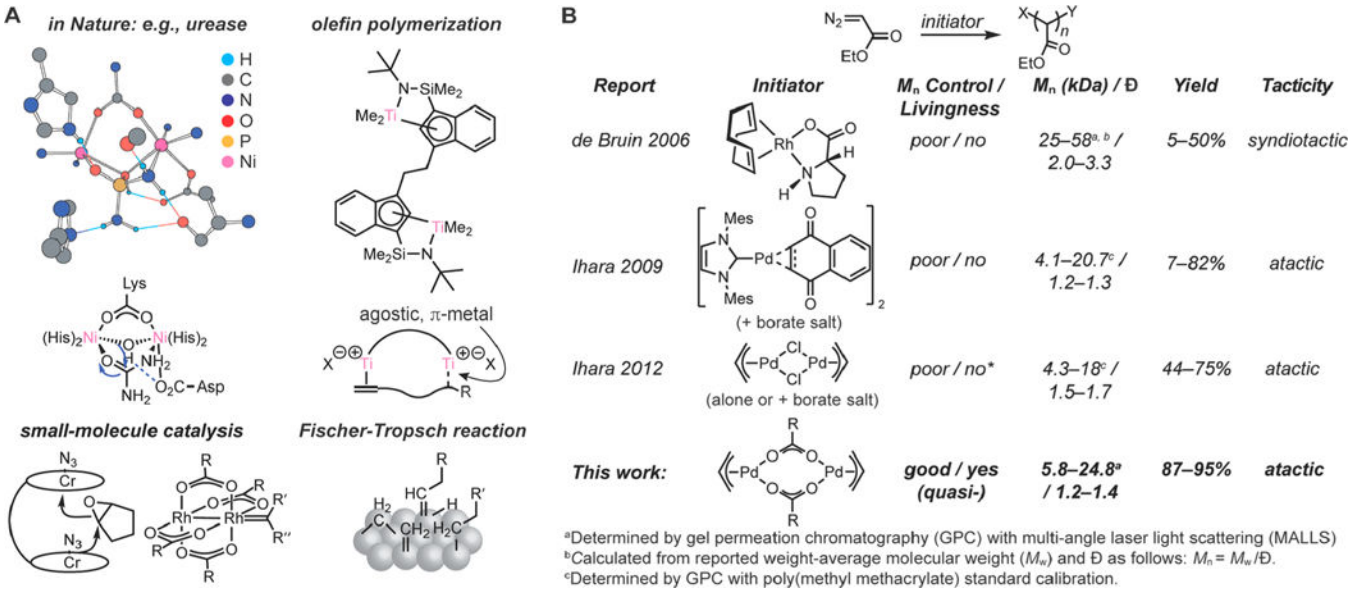


**Figure 1.**

(A) Examples of dinuclear catalysis. Upper left: active site of urease enzyme cocrystallized with diamidophosphoric acid (Reprinted with permission from ref 1. Copyright 1999 Elsevier Ltd.); dinuclear mechanism of urea hydrolysis is provided below.[1] Bottom left: mechanism of a Jacobsen epoxide azidation,[31] and $Rh_2$-carbene structure implicated in a number of carbene transfer reactions.[32] Upper right: example of a dinuclear catalyst for Ziegler—Natta olefin polymerization: agostic or n-metal interactions with one metal center modulate chain transfer at the other.[3] Bottom right: intermediates, including bridging carbenes, believed to be generated in the Fischer—Tropsch reaction.[4] (B) Several literature precedents and this work.[7,26,33] Note that "poor $M_n$ control" refers to insensitivity of the number-average molecular weight $M_n$ to the monomer:initiator ratio. Mes = 2,4,6-trimethylphenyl. *Living behavior was observed for cyclotriphosphazene-containing monomers.[21,22]

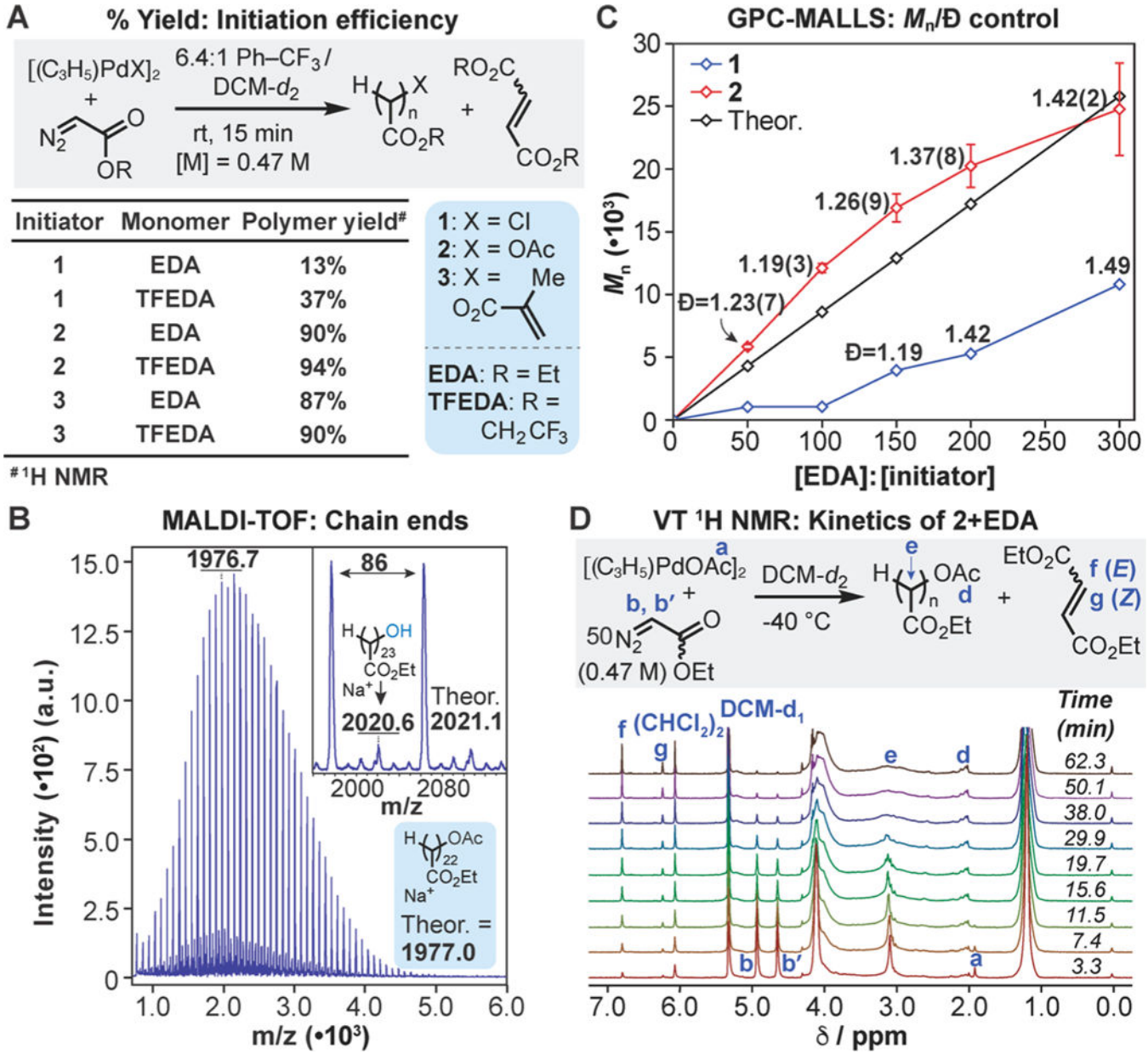


**Figure 2.**

(A) Initiator efficiency as judged by the $^{1}$H NMR yield of polymer. (B) Matrix-assisted laser desorption ionization time-of-flight mass spectrometry (MALDI-TOF MS) of the product of EDA polymerization initiated with **2**. (C) Exploration of $M_n$ control based on the [EDA]:[initiator] ratio (error bars = standard deviations): GPC-MALLS in tetrahydrofuran (THF) at 35 °C was used to analyze polymer samples. Note: for **1**, with [EDA]:[**I**] =50 and 100, $M_n$ is overestimated due to exclusion of the portion of the peak that overlapped with low-$M_n$ species/solvent impurity. (D) EDA polymerization and dimerization mediated by **2** monitored by $^{1}$H NMR spectroscopy ($CD_2Cl_2$, 500 MHz, −40 °C).

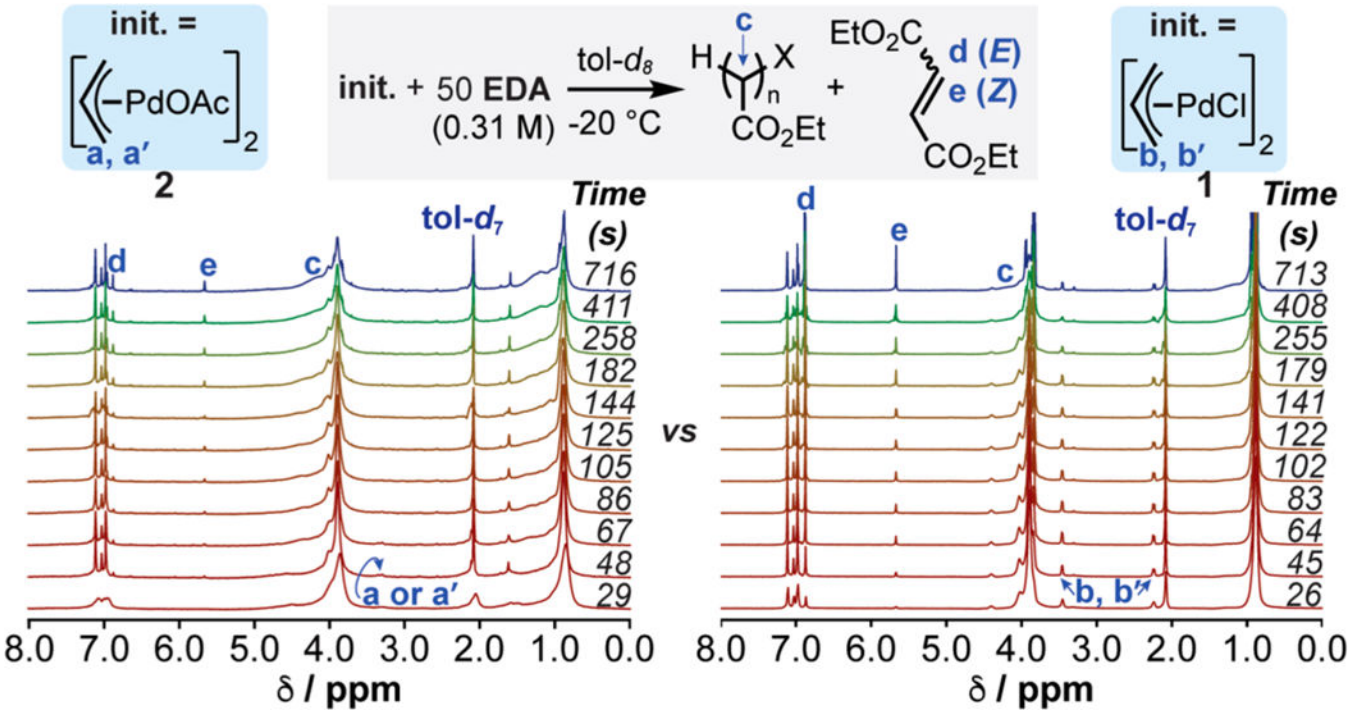


**Figure 3.**

Comparison of initiators **1** and **2** in the polymerization/dimerization of EDA by $^{1}$H rapid-injection (RI)-NMR spectroscopy (toluene-$d_8$,600 MHz, −20 °C).

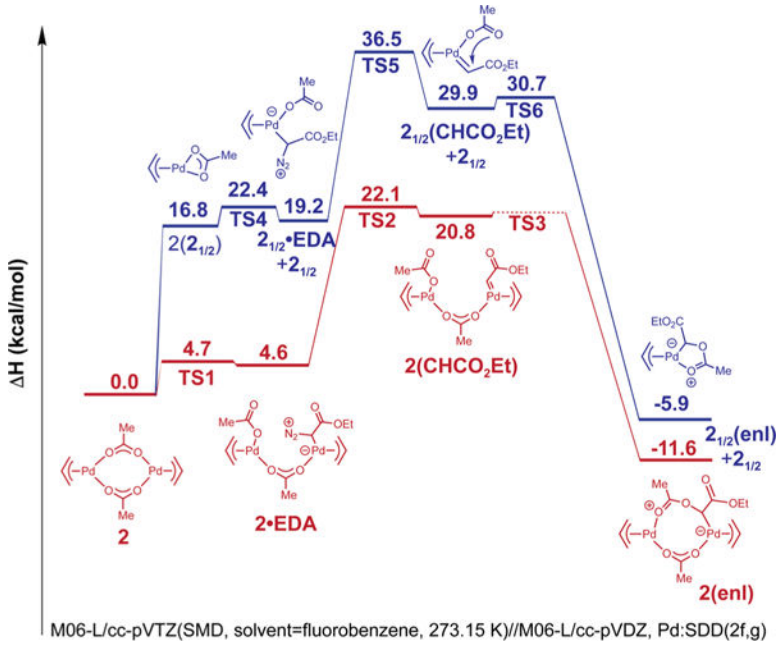


**Figure 4.**

Potential energy diagram calculated via density-functional theory (DFT; level of theory is indicated in the diagram) for the initiation of EDA polymerization with **2** via the mono-and dinuclear pathways (in blue and red, respectively).

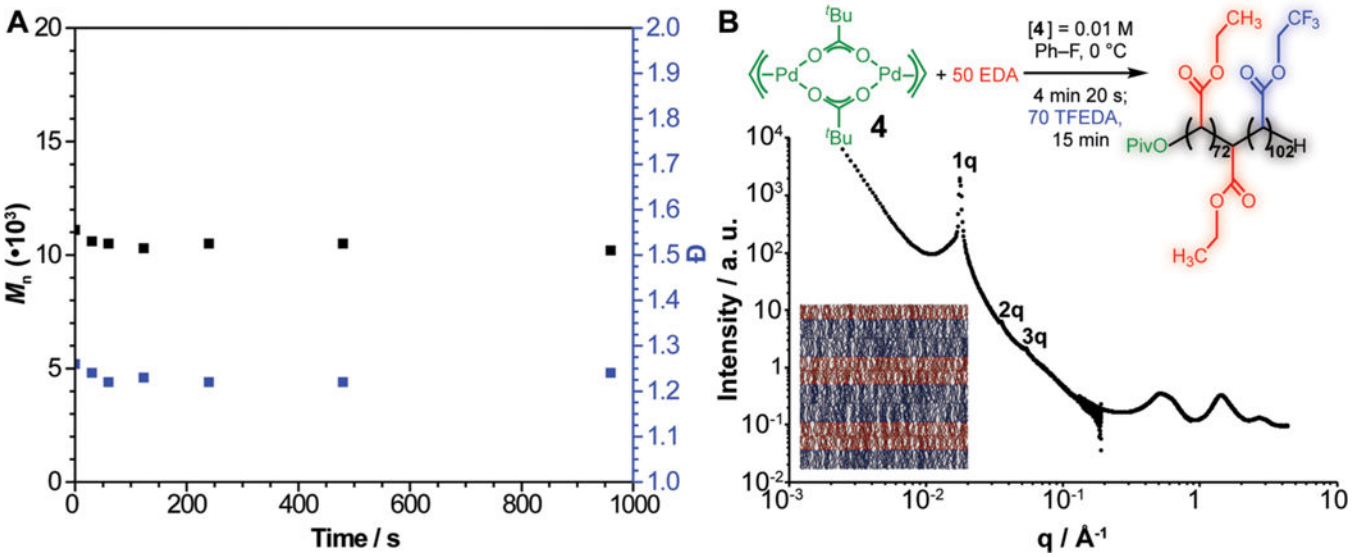


**Figure 5.**

(A) Chain lifetime evaluation for 2/EDA ($M_n$ and D were determined through GPC-MALLS). (B) SAXS/WAXS analysis of the diblock copolymer from EDA and TFEDA formed using initiator 4; illustration of the lamellar morphology is in the bottom left-hand corner.